MARS Axicell Radiation Damage and Shielding Analysis

L. El-Guebaly, L.J. Perkins, and C.W. Maynard

May 1983

UWFDM-506

Nucl. Tech./Fusion **4** (1983) 1171.

FUSION TECHNOLOGY INSTITUTE

UNIVERSITY OF WISCONSIN

MADISON WISCONSIN

MARS Axicell Radiation Damage and Shielding Analysis

L. El-Guebaly, L.J. Perkins, and C.W. Maynard

Fusion Technology Institute
University of Wisconsin
1500 Engineering Drive
Madison, WI 53706

http://fti.neep.wisc.edu

May 1983

UWFDM-506

Nucl. Tech./Fusion 4 (1983) 1171.

MARS AXICELL RADIATION DAMAGE AND SHIELDING ANALYSIS

LAILA EL-GUEBALY
Nuclear Engineering Dept.
1500 Johnson Drive
Madison, Wisconsin 53706
(608) 262-4854

L. JOHN PERKINS
Nuclear Engineering Dept.
1500 Johnson Drive
Madison, Wisonsin 53706
(608) 263-4798

CHARLES MAYNARD
Nuclear Engineering Dept.
1500 Johnson Drive
Madison, Wisconsin 53706
(608) 263-3285

ABSTRACT

Radiation effects and shield requirements are analyzed for the MARS axicell region. Dominant coil life limiting effects in the normal insert coils are found to be swelling in the spinel insulation and resistivity changes of the conductor due to transmutations. The shield between the insert and superconducting coils is optimized and reduces all radiation responses to acceptable levels. However, streaming in the neutral beam duct resulted in an unacceptable dpa rate in the Cu stabilizer and has resulted in a redesign of this region without a neutral beam and with a single insert coil.

INTRODUCTION

The MARS tandem mirror reactor[1] employs a high field axicell to mirror-confine plasma particles without radial drift. This region presents important magnet and shield problems to the designers. The field on axis at the highest point is 24 tesla. Production of this large magnetic field requires the use of a hybrid solenoids where outer superconducting (S/C) coils produce ~ 14 tesla of the required axial field, while inner normal conducting insert coils supply the balance. Figure 1 illustrates the geometric configuration of the axicell coils in the interim version of MARS. The two inner normal conducting coils are positioned with their inner bore behind the first wall with no intervening shielding and are located coaxially with respect to the outer S/C coils. Shielding is placed between the normal and S/C coils and ensures the operational integrity of the latter. Three neutral beam injectors (NBI), evenly distributed around the plasma axis, are located midway between the two S/C coils for plasma fueling and heating of the axicell region.

The radiation transport problem is modeled as an infinite cylinder and discrete ordinates calculations are carried out to investigate the various responses of interest. In the normal coils, there is concern with both electrical and mechanical degradation of the ceramic insulation

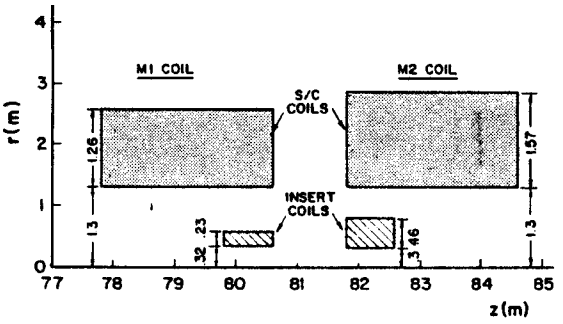

Fig. 1. Geometrical configuration of MARS axicell coils.

and the electrical resistivity of the copper conductor due primarily to transmutations. An additional potential problem is radiolytic decomposition of the water coolant leading to corrosion product formation. Problems of concern in the S/C coils are the dose to the insulators, after the 24 full power years (FPY) designed lifetime of the reactor, heating in the S/C magnet and atomic displacement (dpa) rate in the copper stabilizer of the conductor. The final problem concerns the difficulties of shielding the S/C magnets in the presence of penetrations since clearances are always tight between coils.

RADIATION EFFECTS AND LIFETIME CONSIDERATION FOR THE NORMAL CONDUCTING SOLENOIDS

For economic reasons, the water-cooled normal-conducting insert coils are operated with no intervening shielding between the first wall and their inner windings. In view of the fact that the peak neutron wall load here is 4.5 MWm^{-2}, these magnets will be operating in a severe neutron and gamma radiation environment. It is important, therefore, to recognize potential radiation-induced failure mechanisms so that coil lifetimes can be reasonably predicted.

Accordingly, four potential radiation problem areas were identified as follows:

- Resistivity degradations in the ceramic insulation under instantaneous neutron and gamma absorbed dose-rates.[2]
- Radiolytic dissociation of the coolant water leading to corrosion product formation.
- Mechanical and structural degradations in the ceramic insulation under long-term neutron fluences.
- Resistivity increases in the copper conductor due to radiation damage and neutron-induced transmutations.

Due to space constraints here, only the last two effects will be considered below in that they are potentially lifetime limiting for the current MARS normal-magnet design. All four effects are considered in more detail in an associated paper.[3] However, it should be noted that cognizance of the first two effects exerted a considerable influence on the evolution of early designs of these coils. In particular, extruded conductors with powdered ceramic insulation and externally cooled conductors were rejected due to the potential detrimental consequences of these effects.[3]

Structural Degradation in Ceramic Insulation

To assess the mechanical and structural degradations in the ceramic insulation under elevated neutron fluences, it is necessary to consider two physical characteristics of the material:

- Is the insulator a polycrystalline solid or a compacted powder?
- If the insulator is a solid, does it have a cubic or non-cubic crystal structure?

For compacted powder ceramics, neutron damage has little or no effect on the structural or mechanical properties of the material since each grain is affected individually. In the case of cubic materials (e.g., MgO or $MgAl_2O_4$), swelling is isotropic under neutron irradiation.[4] In fact, the fracture toughness of these materials actually increases under elevated fluences. For example, for a fluence of ~ 2.1 x 10^{26} nm^{-2} (E_n > 0.1 MeV), $MgAl_2O_4$ exhibits swelling of ~ 0.8 vol.% and a strength increase of ~ 20%. Similarly, MgO exhibits swelling of ~ 2.6-3 vol.% and a strength increase of ~ 12-24%.[4] The fluence limit for cubic ceramics is, therefore, determined only by the maximum swelling limit which a particular magnet design can tolerate. However, for non-cubic materials (e.g., Al_2O_3), swelling proceeds anisotropically which leads to the onset of structural microcracking even at modest fluences.[5] These factors dictated the choice of spinel ($MgAl_2O_4$) for the insulation in the normal conducting coils. A reasonable experimental data-base on swelling exists for this material[4] and, to date, appears to offer the lowest degree of swelling among its class of cubic ceramic insulators.

The peak neutron wall loading at the normal magnet is ~ 4.5 MWm^{-2}. From the one-dimensional (1-D) transport calculations, this results in a peak neutron fluence to the spinel of 3.26 x 10^{26} nm^{-2} (E_n > 0.1 MeV) per full power year of operation. The reported neutron swelling data for this material has been for fast fission irradiation and includes < 0.5 vol.% swelling for fluences in the range 2.8 x 10^{25} nm^{-2} to 1.2 x 10^{26} nm^{-2} (E_n > 0.1 MeV) at temperatures of ~ 1000 K, and 0.8 vol.% swelling for irradiation to 2.1 x 10^{26} nm^{-2} (E_n > 0.2 MeV) at T = 430 K.[4] For the particular magnet design under consideration here, 3 vol.% swelling of the insulation was stipulated as a reasonable design limit. Therefore, with the rather conservative assumption that the harder fusion spectrum will enhance the swelling rate by a factor of two over fast fission irradiation, the fluence limit to the spinel insulation was taken to be ~ 2.1 x 10^{26} x (3/0.8) x (1/2) = 3.94 x 10^{26} nm^{-2}.

Resistivity Increases in the Copper Conductor

Resistivity of the copper conductor will increase under neutron irradiation due to two mechanisms, namely:

- Neutron damage via the production of defects and dislocations.
- Production of neutron-induced transmutations leading to the buildup of impurity elements.

The vast majority of work on the effects of neutron damage on copper resistivity has been performed at liquid helium temperatures and stems from interest in copper stabilizers for superconducting magnets. However, two factors combine here to suggest that resistivity effects due to damage are probably small compared with those due to transmutations. First, a large fraction of the defect-induced resistivity which would be encountered at 4.2 K is expected to be self-annealed at the operating temperature

(~ 400 K) of the normal coils[6]; defect resistivity is therefore likely to be small relative to the intrinsic resistivity at this temperature. Second, defect-induced resistivity increases approximately as the square root of the accumulated fluence and lends to a saturation limit at moderately high fluences.[6] In view of the fact that transmutation-induced resistivity scales linearly with fluence, we conclude that defect-induced resistivity is probably only a second-order consideration relative to transmutation effects.

Neutron reactions with the two stable isotopes of copper, ^{63}Cu and ^{65}Cu, give rise to transmutation products. The reactions of interest are (n,p), (n,α), (n,2n) and (n,γ), the latter two resulting in unstable isotopes of copper which subsequently decay to other elements. At any instant of time, neutron transmutations of copper will have produced a mixture of radioactive Co, Ni and Cu isotopes and stable Ni, Zn and Cu isotopes.

A calculation of the number densities of impurity nuclides as a function of radial distance through the largest of the normal conducting coils shown in Fig. 1 was performed as follows. First a 1-D transport calculation of the neutron spectra through the coil was made with the ANISN[7] discrete-ordinates code. The resulting fluxes were then fed to the DKR code[8] which computes time-dependent inventories of radioactive nuclides. Subsidiary calculations were made of stable impurity nuclide inventories using the results from DKR. Impurity concentrations of Co, Ni and Zn were then obtained as a function of radial distance through the coil. At the inner winding, for example, impurity concentrations after 2 FPY operation were 1750 ppm Ni, 971 ppm Zn and 33 ppm Co per MWm^{-2} of neutron wall loading. The resulting radial distribution of resistivity changes in the conductor was then computed from the impurity product concentrations by employing the prescription given by Seitz.[9] Figure 2 shows the resulting resistivity increase in the conductor as a function of radial distance due to these impurities. These increases are after 2 FPY operation and are normalized to a wall loading of 1 MWm^{-2}. From Fig. 2, we see that the maximum resistivity change in the inner winding is ~ 3.23×10^{-9} $\Omega m/MWm^{-2}$ after 2 FPY. Given our peak wall load of ~ 4.5 MWm^{-2} at the coil, we would expect a maximum resistivity change in the inner Zr-Cu winding of ~ 1.55 at an operating temperature of 100°C. Due to the attenuation of the neutron flux with distance through the coil, the resistivity changes are seen to fall off approximately exponentially with a factor of

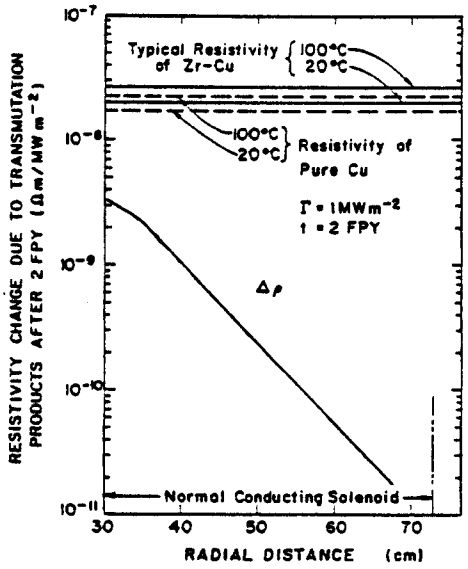

Fig. 2. Radial dependence of resistivity increase in the normal coil due to transmutations.

only ~ 1.004 at the outer winding. The average resistivity change through the coil after 2 FPY is ~ 1.12.

Increasing resistivity with time means increasing power dissipation P in the coil according to $P(t) = I^2R(t)$; note that I must be kept constant to preserve the required ampere-turn conditions. Coil lifetime due to transmutations is, therefore, dependent on the maximum reserve capacity of the magnet power supply (see below).

One other aspect of neutron damage in the copper conductor should be mentioned here. The conductor in the normal magnet has to satisfy two rather conflicting requirements, namely high yield strength against hoop stresses and high electrical conductivity. For these reasons, a number of high strength copper alloys were considered,[3] including MZC (Mg, Zr, Cr, Cu) and AMZIRC (Zr, Cu). Although we have assessed the effects of neutron fluence on conductor resistivity, the consequences of this fluence on conductor ductility and strength is not clear. According to Schultz,[10] there should be no significant loss of ductility in pure copper (or any other FCC material) up to a (fission) fluence of 10^{24} nm^{-2}. However, these recommendations may not necessarily extrapolate to

high strength copper alloys at (fusion) fluences of $> 10^{26}$ nm^{-2}.

Coil Lifetime

Of the four radiation mechanisms likely to degrade the performance of the normal insert coils, only two are seen as lifetime limiting for this particular coil design, namely swelling of the spinel ceramic insulation and neutron-induced transmutations leading to resistivity increases in the conductor. Fluence degradation of the strength of the conductor may be an additional factor.

The fluence limit to the spinel insulation was seen to be ~ 3.94×10^{26} nm^{-2} for the swelling design limit of 3 vol.%.[2] In addition, for a first wall load of 4.5 MWm^{-2}, the peak fluence in the spinel was shown to be ~ 3.26×10^{26} nm^{-2}. Therefore, a lifetime of ~ 1.21 full power years of operation is indicated.

The coil lifetime from a transmutation viewpoint is determined rather critically by the way in which power is supplied to the magnet. The baseline design of the larger of the two normal coils is a set of ~ 23 concentric winding layers, each powered by a separate supply.[1] In this case, the lifetime would be limited by the reserve margin of the supply feeding the inner winding. For example, for a supply with a 50% reserve margin, the coil would require replacement every 1.82 FPY since the resistivity of the inner winding was seen to increase by a factor of 1.55 after 2 FPY. However, at this time a design change is contemplated in which the whole winding length would be powered by one supply. In this case, the power supply margin after two full power years would only need to compensate for the average increase in resistivity of the coil, i.e. ~ 12%. Therefore, providing the increased Joule heating in the inner windings can be accommodated, this latter design should ensure long coil life with regard to conductor resistivity increases.

One other interesting feature of increasing coil resistivity is the associated increasing operating costs. Depending on the particular coil design under consideration, the normal Joule heating losses are ~ 45 MW per coil at start of life.[3] Taking electricity costs to be ~ 5¢/kWh, a resistivity increase of 12% over 2 FPY of operation represents an additional operating cost of ~ 2.4 M$ per coil, a not inconsequential amount!

At present, therefore, the lifetime of this highly irradiated coil appears to be limited by swelling of the spinel insulation to ~ 1.21 full power years.

SHIELD OPTIMIZATION

In order to keep the S/C coils as small as possible, the shield is optimized for the three most important responses mentioned before. The left corner of the first mirror (M1) S/C coil has the most severe radiation effects. At this corner, the shield is constrained to 0.75 m in addition to 0.2 m thick coil case and cryostat. In this regard, the use of tungsten in the shield is essential to provide adequate protection of the S/C magnet from the intense neutron source (3.7 MW/m^2 wall loading) and gamma radiation. The shield was configured originally in three layers. First, a W-layer (80 vol.% W [90% d.f.], 10 vol.% Fe 1422 and 10 vol.% H_2O) to effectively slow down the high energy neutrons; next, a B_4C-layer (86 vol.% B_4C [87% d.f.], 10 vol.% Fe 1422 and 4 vol.% H_2O) to moderate the neutrons further and absorb the low energy neutrons; and finally, a thin lead layer (86 vol.% Pb, 10 vol.% Fe 1422 and 4 vol.% H_2O) to reduce the gamma heating in the magnet. The primary motive for the optimization study is to find an optimal combination of the W, B_4C and lead layers that minimizes the dpa rate in the Cu stabilizer which was found to be the design driver for the shield. In order to limit anneals of the S/C magnet, a limit of 1.9×10^{-4} dpa after 5 FPY has been adopted. Other limits of interest are the dose in the electrical insulator (GFF polyimide) and the peak power density in the S/C magnet.[3] These are taken as 5×10^9 rad and 0.06 mW/cm^3, respectively.

A series of 1-D calculations was performed to determine the optimal shield configuration using the discrete ordinates code ONEDANT,[11] the cross section library XSLIB (30 neutron and 12 gamma energy groups) based on the ENDF/B-V evaluation, and the P_3-S_8 approximation in cylindrical geometry. The optimization study was performed in several steps. First, the lead layer was varied in thickness and the proportion of the W-layer to the B_4C layer thickness was kept the same. Figure 3 indicates that the lead layer is not helping significantly and a shield consisting of B_4C and W is more effective in reducing the dpa rate in Cu. Second, the thickness of the B_4C layer was varied under the constraint that the total shield thickness remains 0.75 m. The result was that 0.73 m of W-layer backed by 0.02 m B_4C layer is the optimal combination (as shown in Fig. 4) that minimizes the dpa rate. Finally, the 10 vol.% water content in the W-layer was found to be an optimal value. The optimal combination actually provided more

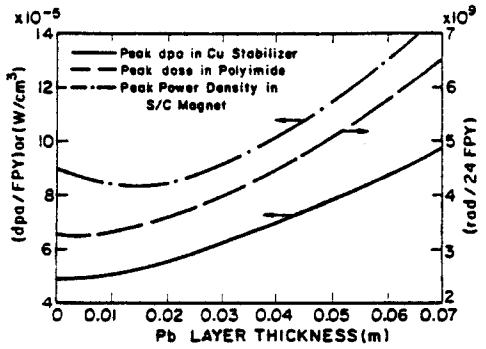

Fig. 3. Variation of the radiation damage in the S/C magnet with the Pb layer thickness.

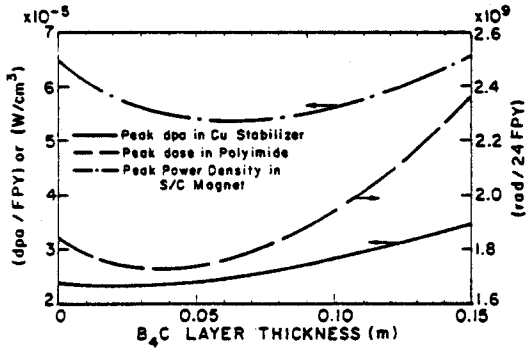

Fig. 4. Variation of the radiation damage in the S/C magnet with the B_4C layer thickness.

shielding than the design goals and to make the shield somewhat less expensive without redesigning the magnets, the tungsten in the last 0.14 m of the W-layer was replaced by the Fe 1422 steel.

Some observations can be made from the results of the optimization scheme. The optimal combination that minimizes the radiation effects in the S/C magnet may vary from one response to the other. The lead can back up the shield if the heating in the S/C magnet is the response of interest. The optimal combination of W and B_4C layers demonstrates the dominance of tungsten in decreasing the dpa rate.

NEUTRONICS ANALYSIS OF THE NBI DUCT SHIELD

In MARS the neutral beams were introduced between the split axicell S/C and insert coils. This creates a shielding problem as neutrons stream up the ducts and produce excessive radiation damages in the front corner of the S/C coil. The NBI ducts were oriented at 90° to the axis and the duct opening of 0.325 x 0.48 m looked directly at the peak neutron source creating a maximum wall loading of 4 MW/m^2 at a 0.30 m first wall radius. At the point on the duct wall nearest the front corner of the S/C coil, a space of only 0.3375 m was available for shielding besides a 0.058 m equivalent thickness of steel provided by the magnet case and cryostat. A first cut estimate was made for the required shield to adequately protect the S/C magnet by calculating the wall loading at the point on the duct wall nearest the front corner of the S/C coil. This was found to be 2.3 x 10^{-2} MW/m^2. A subsequent 1-D calculation indicated that at least 0.463 m of shield is required and the three-dimensional (3-D) calculations confirmed the estimate as will be shown later.

In order to assess the shielding problem posed by the NBI ducts, a 3-D radiation transport model was implemented using the Monte Carlo Code MCNP[12] and ENDF/B-V data library. Trapping surfaces were located at the entrances of the NBI ducts where all crossing particles are counted according to energy and angle bins. This information was served as a surface source in the modeling of the NBI duct itself. The geometrical configuration of the NBI duct is shown in Fig. 5 where only the corner of the M1 coil was modeled as radiation damage effects in other parts of the S/C magnet are less severe. In order to reduce the statistical uncertainties below 50% in the quantities of interest, the angle of source neutrons was biased toward the corner of the S/C magnet, and splitting surfaces were used to increase the number of particles as they move in the direction of interest. Also the particles were forced to have at least one collision in the S/C magnet region.

The calculational results of 20,000 histories indicate a peak dpa in the Cu stabilizer of 3.6 x 10^{-4} dpa/FPY. Thus the shield is inadequate on this basis. An estimate was made as to the required shield to protect the S/C magnet leading to a need for 0.455 m shield based on 1/10 folding distance of ~ 0.12 m for the optimized shield. These results were a major contributing factor to the abandonment of the use of neutral beam injection and split S/C coil in later versions of MARS. The most recent design of MARS employs a single insert coil located coaxially with a single S/C coil which has an inner bore radius of 1.4 m to accommodate for more radiation shield.

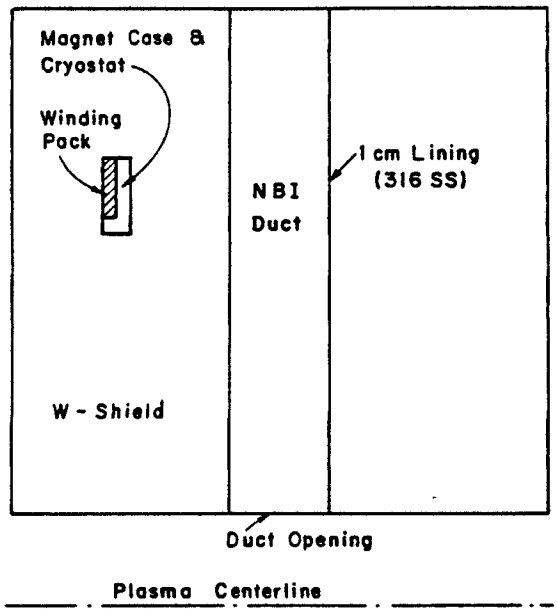

Fig. 5. Geometrical model of MARS axicell NBI duct for MCNP calculations.

CONCLUSIONS

Radiation effects have had a major impact on design changes to the axicell region in the MARS tandem mirror reactor. In particular, identification of damage to the superconducting coils from neutron streaming has resulted in the removal of the neutral beam duct and combination of the split coils. These effects also create one of the most difficult maintenance tasks due to the necessity of replacing the insert coils every 1.2 FPY, i.e. less than two calendar years. Further design changes could increase the changeout period.

ACKNOWLEDGMENT

The authors would like to acknowledge the work performed by A.M. White and W.F. Vogelsang in their assistance with the DKR radioactivity code.

REFERENCES

1. "Mirror Advanced Reactor Study (MARS) - Interim Report," UCRL-53333, Lawrence Livermore National Laboratory (to be published 1983).

2. L.J. PERKINS, "Radiation Dose-Rate Resistivity Degradation in Ceramic Insulators and Assessment of the Consequences in Fusion Reactor Applications," UWFDM-469, University of Wisconsin Fusion Engineering Program Report (1982).

3. L.J. PERKINS, "Materials Considerations for Highly Irradiated Normal-Conducting Magnets." To be submitted to 5th Topical Meeting on Fusion Reactor Materials, Albuquerque, NM, September 1983.

4. G.F. HURLEY, J.C. KENNEDY and F.W CLINARD, "Structural Properties of MgO and $MgAl_2O_4$ After Fission Neutron Irradiation Near Room Temperature," LA-UR 81-2078, Los Alamos Scientific Laboratory (1981).

5. F.W. CLINARD, "Ceramics for Applications in Fusion Systems," *J. Nucl. Mater.*, *85 & 86*, 393 (1979).

6. J.M. WILLIAMS, C.E. KLABUNDE, J.K REDMAN, R.R. COLTMAN and R.L. CHAPLIN, "The Effects of Irradiation on the Copper Normal Metal of a Composite Superconductor," *IEEE Trans. Mag., MAG-15*, 731 (1979).

7. "ANISN-ORNL," RSIC Code Package CCC-254, Radiation Shielding and Information Center, Oak Ridge National Laboratory (1979).

8. T.Y. SUNG and W.F. VOGELSANG, "DKR: A Radioactivity Calculation Code for Fusion Reactors," UWFDM-170, University of Wisconsin Fusion Engineering Program Report (1976).

9. F. SEITZ, *The Modern Theory of Solids*, p. 41, McGraw-Hill (1940).

10. J.H. SCHULTZ, "Design Practice and Operational Experience of Highly Irradiated High Performance Normal Magnets" PFC/RR-82-25, p. 27, MIT Plasma Fusion Center (1982).

11. R.D. O'DELL et al.,"User's Manual for ONEDANT: A Code Package for One-Dimensional, Diffusion-Accelerated, Neutral-Particle Transport," Los Alamos National Laboratory LA-9184-M (1982).

12. Los Alamos Monte Carlo Group X-6, "MCNP - A General Monte Carlo Code for Neutron and Photon Transport," LA-7396-M (1981).